

Fuzzy dark matter
(Ultralight axion dark matter)

Lam Hui 許林
Columbia University

Outline

- High energy physics considerations - natural cosmic abundance.
- Basic dynamics - a superfluid with quantum pressure/stress.
- Astrophysical implications - dynamical friction, tunneling, interference, etc.

Collaboration with Jerry Ostriker, Scott Tremaine and Edward Witten.

Ultralight scalar dark matter

$$\text{mass } m \sim 10^{-22} \text{ eV}$$

$$(mv)^{-1} \sim 2 \text{ kpc } (10 \text{ km s}^{-1}/v)$$

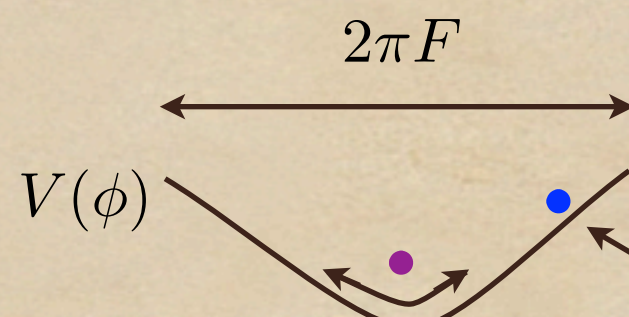
- A natural candidate for such a light particle is a pseudo Goldstone boson.
- Concrete realization: an angular field of periodicity $2\pi F$ i.e. an axion-like field with a potential from non-perturbative effects (not QCD axion).

$$\mathcal{L} \sim -\frac{1}{2}(\partial\phi)^2 - \underbrace{\Lambda^4(1 - \cos[\phi/F])}_{V(\phi)}$$

$$m \sim \Lambda^2/F$$

- Relic abundance:

(standard story - see review by Marsh)



$$\ddot{\phi} + 3H\dot{\phi} = -V'(\phi)$$

subsq. oscill. : $\rho_\phi \propto a^{-3}$
 self - interaction can be ignored

$\phi \sim F$ at early times until $H \sim m$
 $\rho_\phi \sim m^2 F^2$, $\rho_{\text{rad.}} \sim H^2 M_{\text{pl}}^2$

$$\Omega_{\text{matter}} \sim \left(\frac{F}{10^{17} \text{ GeV}} \right)^2 \left(\frac{m}{10^{-22} \text{ eV}} \right)^{1/2}$$

(Note : 1. $\Lambda \sim 100 \text{ eV} \left(\frac{m}{10^{-22} \text{ eV}} \right)^{1/2} \left(\frac{F}{10^{17} \text{ GeV}} \right)^{1/2}$; 2. low scale inflation)

Dynamics of a free massive scalar

- Ignoring self-interaction:

$$-\square\phi + m^2\phi = 0$$

$$m^{-1} \sim 0.06 \text{ pc}$$

$$(mv)^{-1} \sim 2 \text{ kpc } (10 \text{ km s}^{-1}/v)$$

- Non-relativistic limit:

$$\phi = \frac{1}{\sqrt{2m}} [\psi e^{-imt} + \psi^* e^{imt}]$$

$$|\ddot{\psi}| \ll m|\dot{\psi}| \longrightarrow i\dot{\psi} = \left[-\frac{\nabla^2}{2m} + m\Phi_{\text{grav.}} \right] \psi$$

- High occupancy implies ψ should be thought of as a classical scalar. See simulations by Hsi-Yu Schive, Tzihong Chiueh & Tom Broadhurst.
- An alternative viewpoint: ψ as a (classical) fluid.

$$\rho = m|\psi|^2 \quad \text{i.e.} \quad \psi = \sqrt{\rho/m} e^{i\theta}$$

Recall conservation of probability: current $\propto i(\psi\nabla\psi^* - \psi^*\nabla\psi)$

Reinterpreted as conservation of mass:

$$\dot{\rho} + \nabla \cdot \rho v = 0 \quad \text{where} \quad v = \frac{1}{m} \nabla \theta \quad \text{i.e. a superfluid.}$$

Fluid formulation (Madelung)

- Euler equation:

$$\dot{v} + v \cdot \nabla v = -\nabla \Phi_{\text{grav.}} + \frac{1}{2m^2} \nabla \left(\frac{\nabla^2 \sqrt{\rho}}{\sqrt{\rho}} \right)$$

↑
“quantum pressure”

- More precisely, an unusual form of stress:

$$T_{ij} = \rho v_i v_j + \frac{1}{2m^2} [\partial_i \sqrt{\rho} \partial_j \sqrt{\rho} - \sqrt{\rho} \partial_i \partial_j \sqrt{\rho}]$$

- Can be implemented in standard hydrodynamics codes (Mocz & Succi).
- For linear perturbations (on cosmological bgd.):

$$\text{Jeans scale} \sim 0.1 \text{ Mpc}$$

Perturbations suppressed on small scales - could help avoid small scale problems of standard CDM (Hu, Barkana, Gruzinov: **Fuzzy DM**; Amendola, Barbieri).

Typical focus: density profile (cusp versus core), number of satellite galaxies.

Issue: baryonic effects make it hard to draw definitive conclusions.

The unexpected diversity of dwarf galaxy rotation curves

Kyle A. Oman^{1,*}, Julio F. Navarro^{1,2}, Azadeh Fattahi¹, Carlos S. Frenk³,
Till Sawala³, Simon D. M. White⁴, Richard Bower³, Robert A. Crain⁵,
Michelle Furlong³, Matthieu Schaller³, Joop Schaye⁶, Tom Theuns³

¹ *Department of Physics & Astronomy, University of Victoria, Victoria, BC, V8P 5C2, Canada*

² *Senior CIFAR Fellow*

³ *Institute for Computational Cosmology, Department of Physics, University of Durham, South Road, Durham DH1 3LE, United Kingdom*

⁴ *Max-Planck Institute for Astrophysics, Garching, Germany*

⁵ *Astrophysics Research Institute, Liverpool John Moores University, IC2, Liverpool Science Park, 146 Brownlow Hill, Liverpool, L3 5RF, United Kingdom*

⁶ *Leiden Observatory, Leiden University, PO Box 9513, NL-2300 RA Leiden, the Netherlands*

10 July 2015

ABSTRACT

We examine the circular velocity profiles of galaxies in Λ CDM cosmological hydrodynamical simulations from the EAGLE and LOCAL GROUPS projects and compare them with a compilation of observed rotation curves of galaxies spanning a wide range in mass. The shape of the circular velocity profiles of simulated galaxies varies systematically as a function of galaxy mass, but shows remarkably little variation at fixed maximum circular velocity. This is especially true for low-mass dark matter-dominated systems, reflecting the expected similarity of the underlying cold dark matter haloes. This is at odds with observed dwarf galaxies, which show a large diversity of rotation curve shapes, even at fixed maximum rotation speed. Some dwarfs have rotation curves that agree well with simulations, others do not. The latter are systems where the inferred mass enclosed in the inner regions is much lower than expected for cold dark matter haloes and include many galaxies where previous work claims the presence of a constant density “core”. The “cusp vs core” issue is thus better characterized as an “inner mass deficit” problem than as a density slope mismatch. For several galaxies the magnitude of this inner mass deficit is well in excess of that reported in recent simulations where cores result from baryon-induced fluctuations in the gravitational potential. We conclude that one or more of the following statements must be true: (i) the dark matter is more complex than envisaged by any current model; (ii) current simulations fail to reproduce the diversity in the effects of baryons on the inner regions of dwarf galaxies; and/or (iii) the mass profiles of “inner mass deficit” galaxies inferred from kinematic data are incorrect.

Key words: dark matter, galaxies: structure, galaxies: haloes

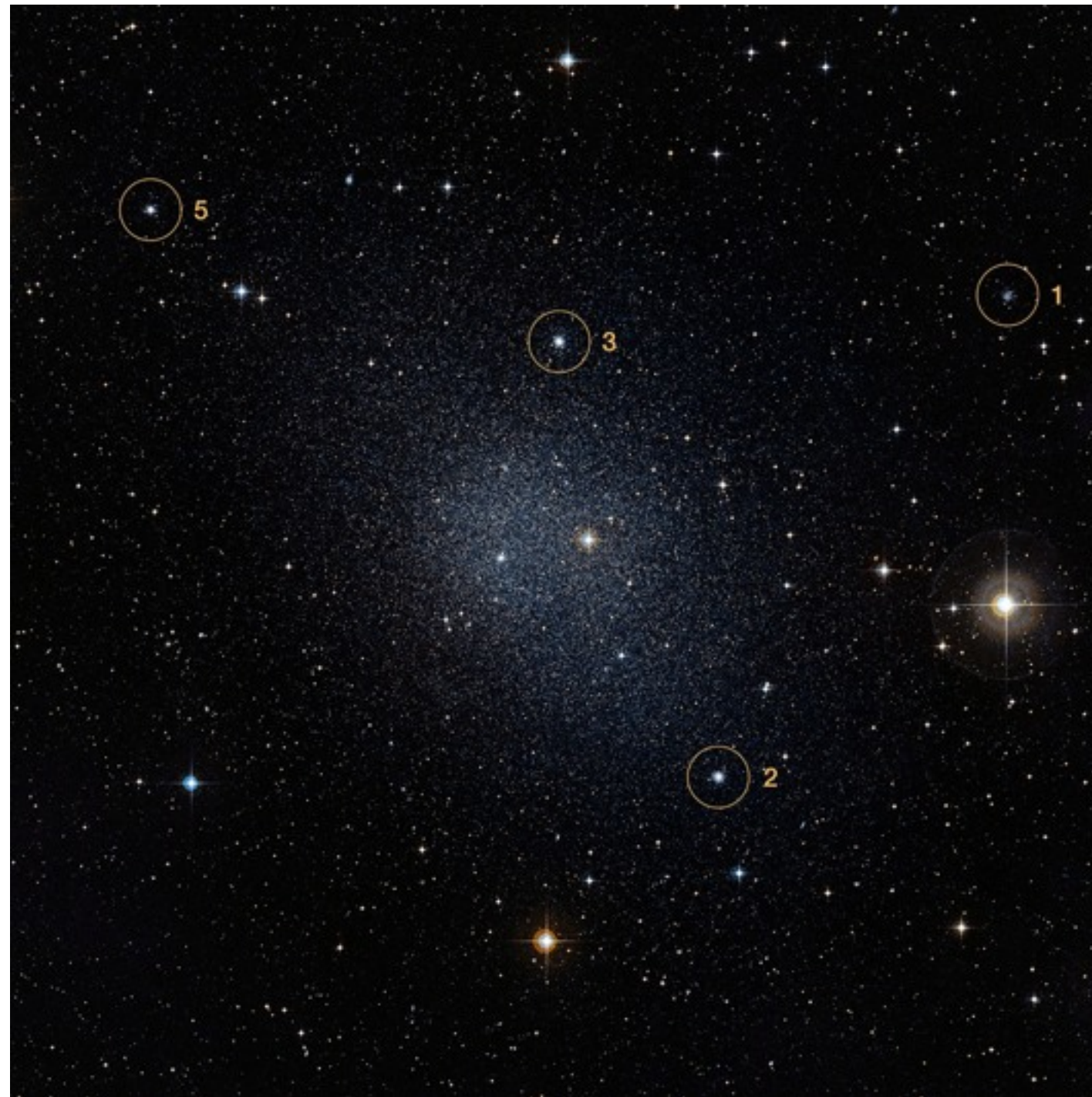
arXiv:1504.01437v2 [astro-ph.GA] 9 Jul 2015

Possible diagnostics of FDM vs conventional CDM:

- dynamical friction
- evaporation of sub-halos by tunneling
- interference
- tidal streams and gravitational lensing
- Lyman-alpha forest
- direct detection
- detection by pulsar timing array

Fornax galaxy and its globular clusters

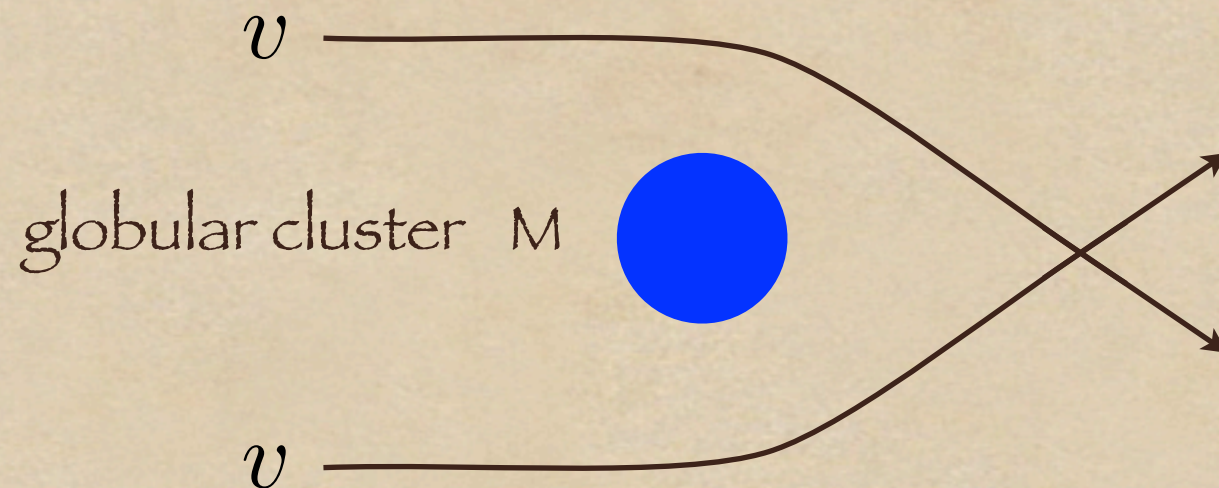
ESO/Digitized Sky Survey 2



Dynamical friction issue: Tremaine 1976

Dynamical friction

- Chandrasekhar's classic calculation:



- Quantum stress smooths out density wake, lowering friction. (see also Lora et al.)
- Use known solution for the Coulomb scattering problem:
$$\psi \propto F [i\beta, 1, ikr(1 - \cos \theta)]$$
 where F is the confluent hypergeometric func.
$$\beta \equiv (GM/v^2)/k^{-1}$$
 with $k^{-1} = (mv)^{-1} = \text{de Broglie wavelength}$

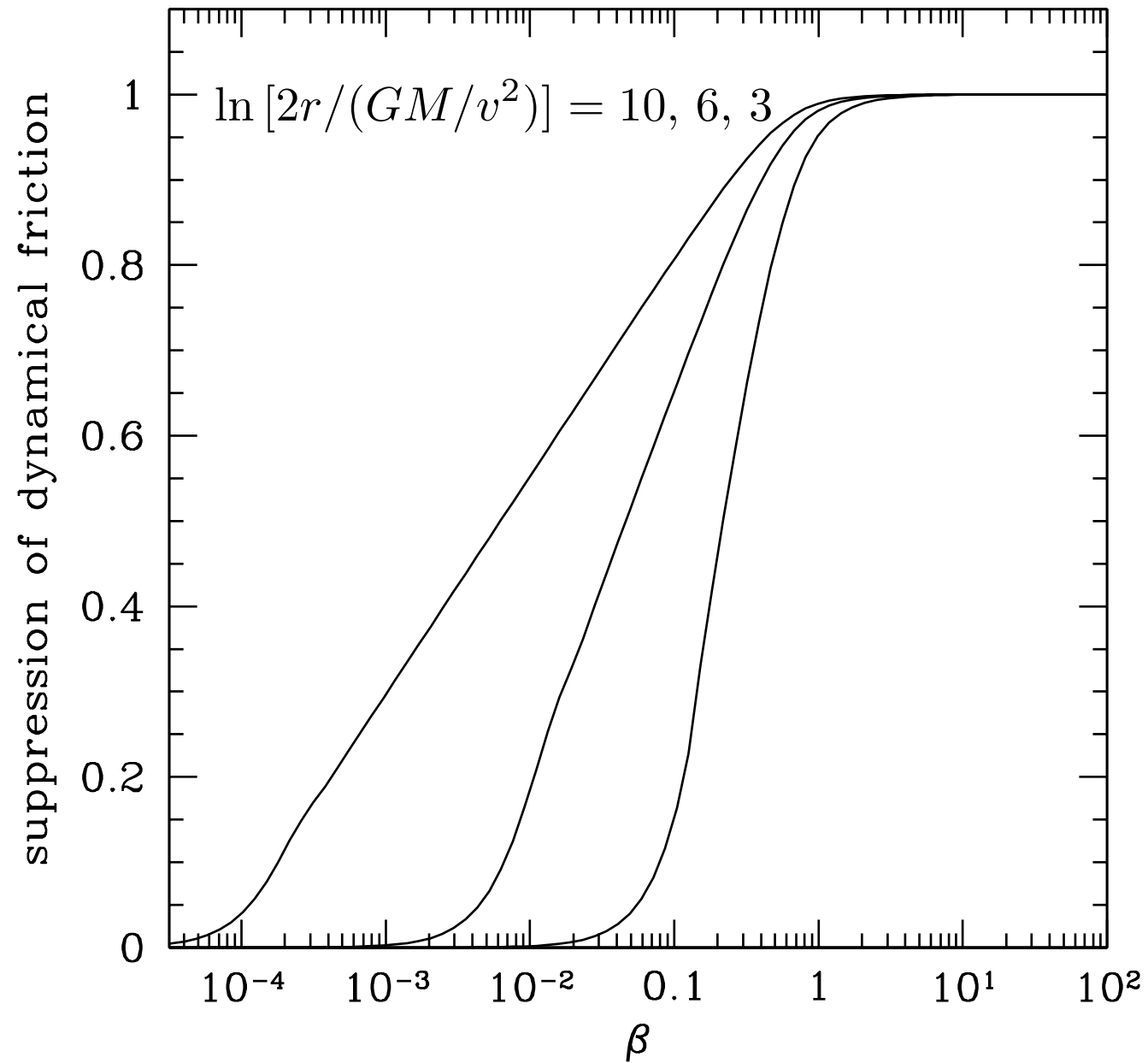
Small β means quantum stress is important.

- **Key** - integrate momentum flux to compute friction: $\oint dS_j T_{ij}$

Question: shouldn't the quantum and classical answers be identical?

Recall that for Coulomb differential cross section,
quantum = classical.

- But recall also the integrated cross section has a logarithmic divergence.
- Thus, we expect dynamical friction $\propto \ln [r/r_c]$ where $r \sim$ size of galaxy,
 $r_c \sim GM/v^2$ or k^{-1}
- This is borne out by analytic calculation, made possible by obscure identities involving hypergeometric functions.



$$\beta \equiv (GM/v^2)/k^{-1}$$

$$= 0.0023 \left(\frac{M}{10^5 M_\odot} \right) \left(\frac{10 \text{ km/s}}{v} \right) \left(\frac{m}{10^{-22} \text{ eV}} \right)$$

Conclusion on dynamical friction:

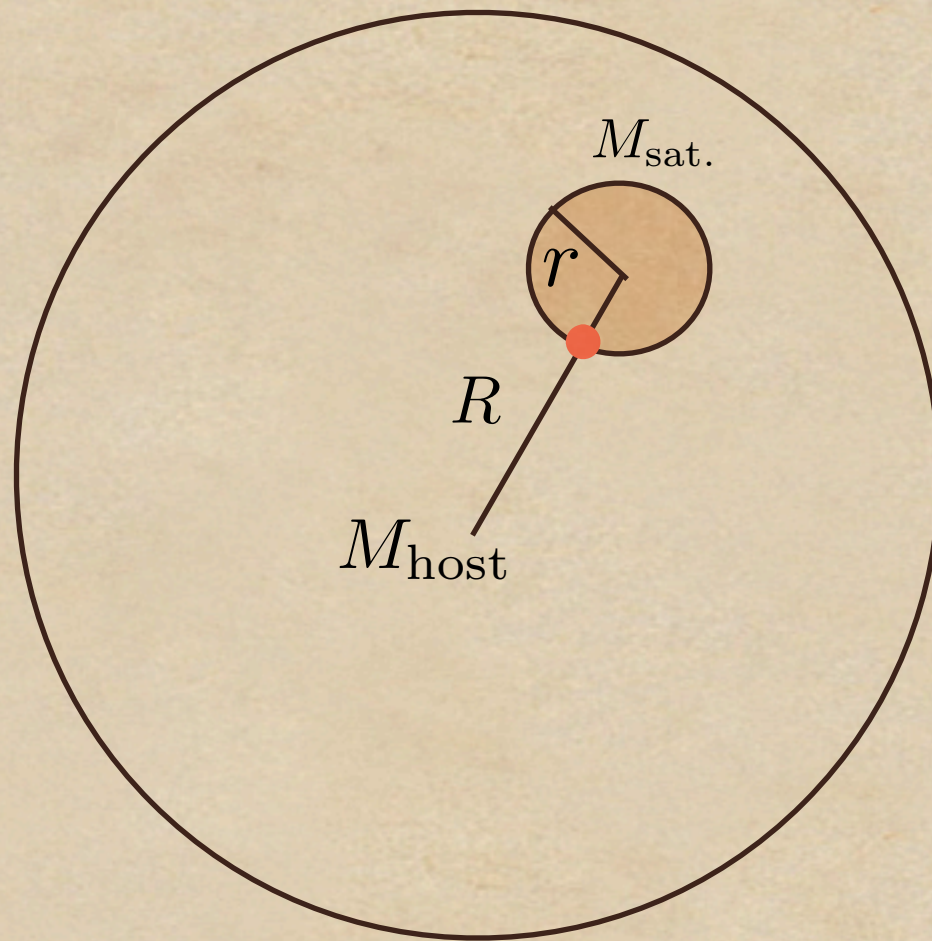
Given the density profile of a galaxy (which can be experimentally determined), standard CDM has a definite prediction for the dynamical friction, which can be checked against observations.

Fuzzy DM of $m \sim 10^{-22}$ eV can lower dynamical friction by an order of magnitude.

Would be useful to study other systems: Lotz et al. 2001

Possible diagnostics of FDM vs CDM:

- dynamical friction ✓
- evaporation of satellites by tunneling
- tidal streams & gravitational lensing
- globular cluster formation
- Lyman-alpha forest
- direct detection
- detection by pulsar timing array

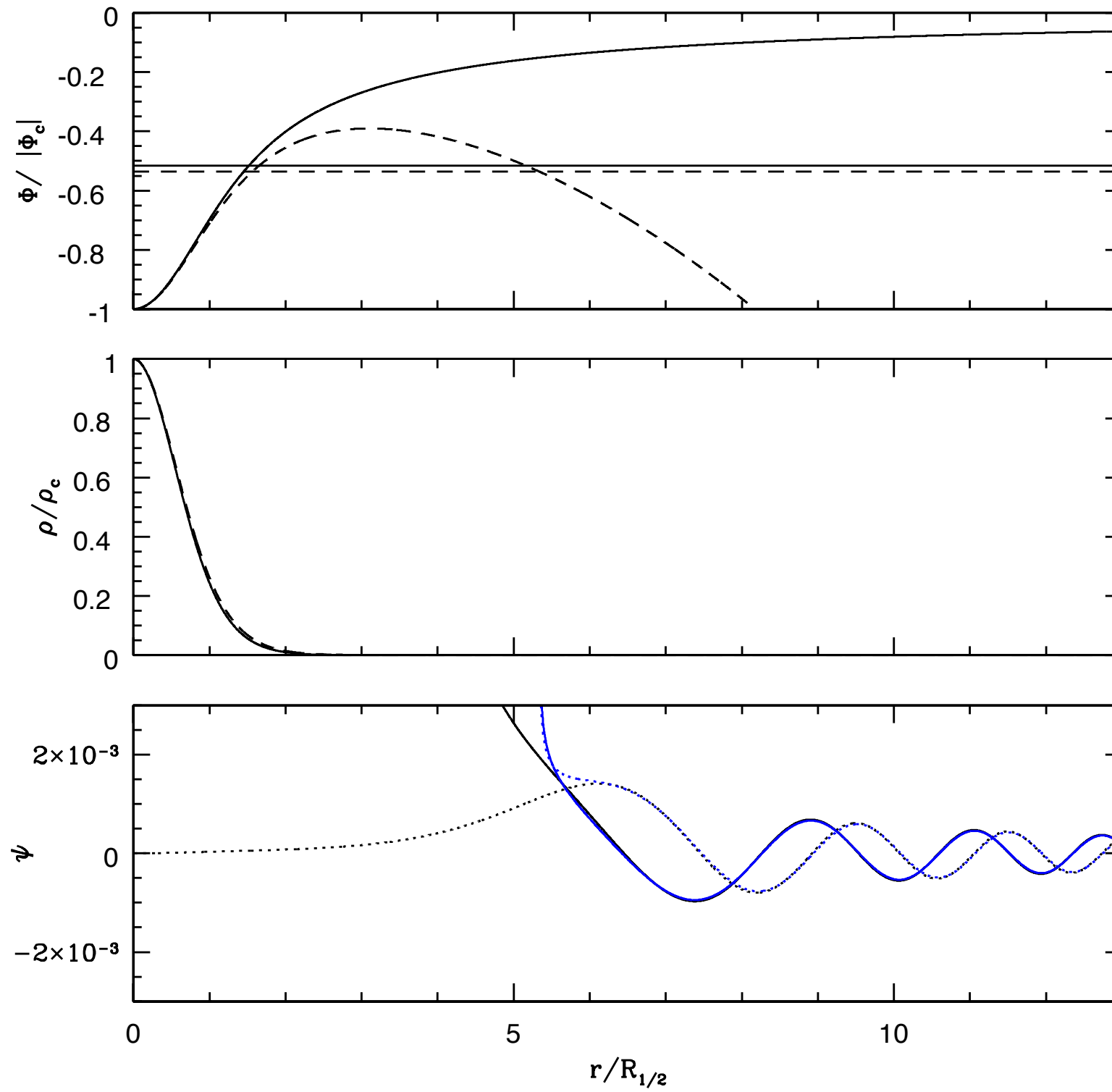


Recall tidal disruption: $\frac{GM_{\text{host}}}{R^2} \frac{r}{R} \sim \frac{GM_{\text{sat.}}}{r^2}$

$r =$ disruption radius

Quantum pressure is expected to alter this.

$M_{\text{satellite}} > 10^8 M_{\odot}$ in Milky Way



Possible diagnostics of FDM vs CDM:

- dynamical friction ✓
- evaporation of satellites by tunneling ✓
- interference
- tidal streams & gravitational lensing
- Lyman-alpha forest
- direct detection
- detection by pulsar timing array

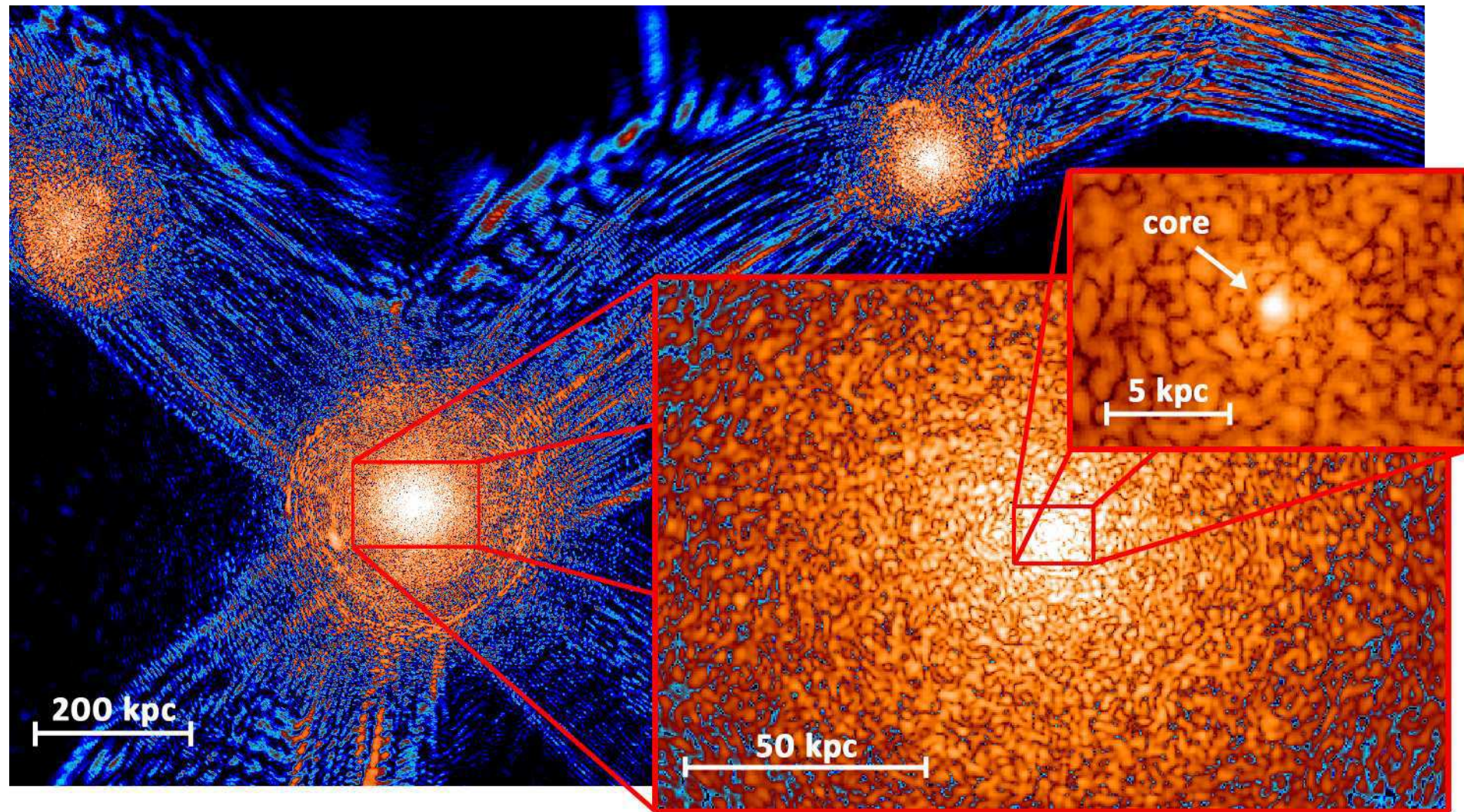
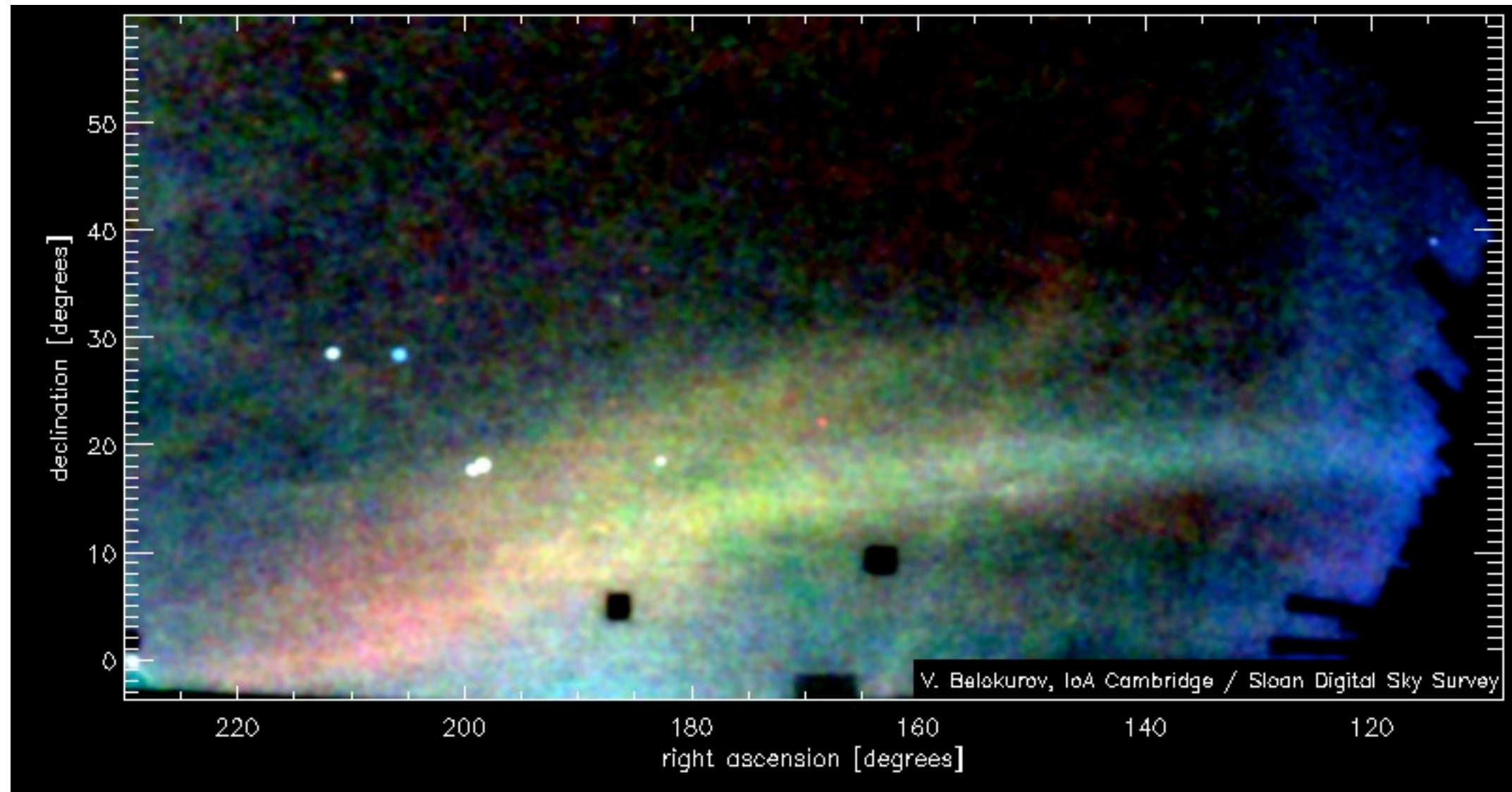
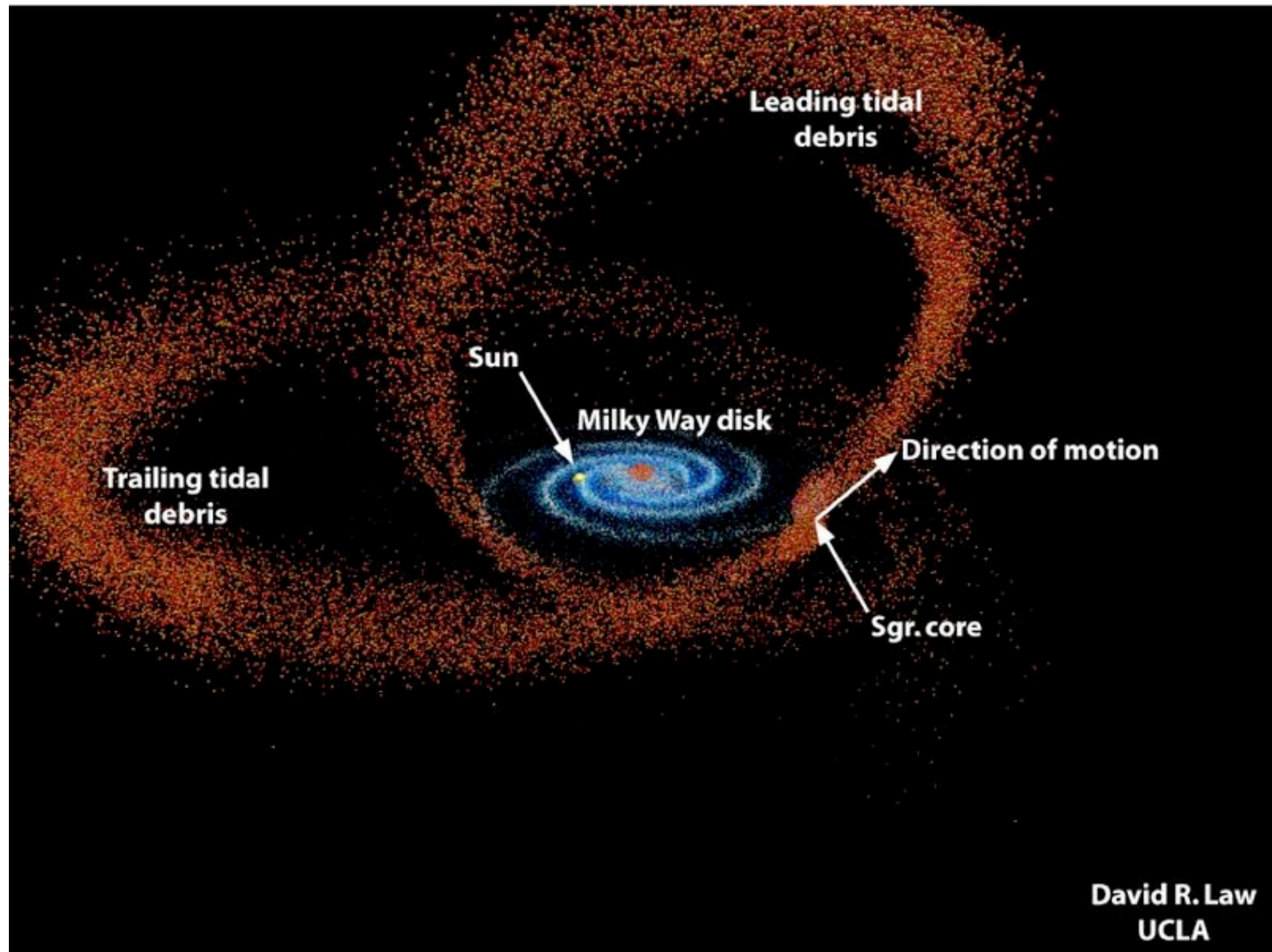


Figure 2: A slice of density field of ψ DM simulation on various scales at $z = 0.1$. This scaled sequence (each of thickness 60 pc) shows how quantum interference patterns can be clearly seen everywhere from the large-scale filaments, tangential fringes near the virial boundaries, to the granular structure inside the haloes. Distinct solitonic cores with radius $\sim 0.3 - 1.6$ kpc are found within each collapsed halo. The density shown here spans over nine orders of magnitude, from 10^{-1} to 10^8 (normalized to the cosmic mean density). The color map scales logarithmically, with cyan corresponding to density $\lesssim 10$.

Schive, Chiueh, Broadhurst



Belokurov, Zucker et al. SDSS II data



Law, Majewski, Johnston model of Sagittarius stream

Possible diagnostics of FDM vs CDM:

- dynamical friction ✓
- evaporation of satellites by tunneling ✓
- interference ✓
- tidal streams & gravitational lensing ✓
- Lyman-alpha forest
- direct detection
- detection by pulsar timing array

Outline

- High energy physics considerations - natural cosmic abundance.
- Basic dynamics - a superfluid with quantum pressure/stress.
- Astrophysical implications - dynamical friction, tunneling, interference, etc.

Collaboration with Jerry Ostriker, Scott Tremaine and Edward Witten.

Extra slides follow.

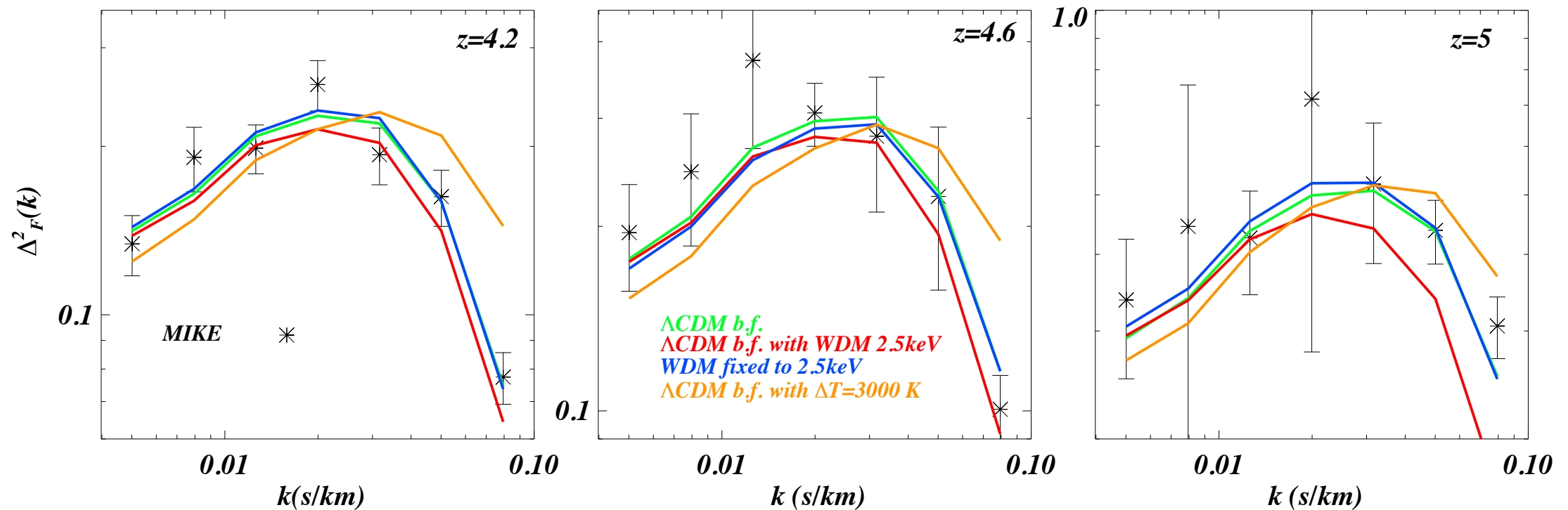


FIG. 11: The best fit model for the MIKE data set (black crosses) used in the present analysis, shown as the green curves and labelled as “ Λ CDM b.f.”. This model is very close to Λ CDM. We also show for qualitative purposes a few other models: a WDM model that has the same parameters as the best fit model except for the WDM mass (red curves) which is chosen to be 2.5 keV; a model that has a hotter temperature (orange curves) and a model for which the mass of the WDM is fixed to $m_{\text{WDM}} = 2.5$ keV, but for which all other parameters are set to their best-fitting values for this choice (blue curves). Note that for the MIKE data we do not use the $z = 5.4$ redshift bin.

Naive translation : $m_{\text{WDM}} \sim 2.5 \text{ keV} \rightarrow m_{\text{FDM}} \sim 10^{-21} \text{ eV}$

- But :
- allowing non – monotonic thermal history relaxes WDM mass bound by 1 keV (Garzilli et al.)
 - fluctuations in the ionizing background and reionization history could be important
 - granularity of FDM might be non – negligible

Possible diagnostics of FDM vs CDM:

- dynamical friction ✓
- evaporation of satellites by tunneling ✓
- interference ✓
- tidal streams & gravitational lensing ✓
- Lyman-alpha forest ✓
- direct detection
- detection by pulsar timing array

Pulsar timing signal from ultralight scalar dark matter

Andrei Khmelnitsky^a and Valery Rubakov^{b,c}

^a*Arnold Sommerfeld Center for Theoretical Physics,
Ludwig Maximilians University,
Theresienstr. 37, 80333 Munich, Germany*

^b*Institute for Nuclear Research of the Russian Academy of Sciences,
60th October Anniversary Prospect, 7a, 117312 Moscow, Russia*

^c*Department of Particle Physics and Cosmology, Physics Faculty,
M.V. Lomonosov Moscow State University,
Vorobjevy Gory, 119991, Moscow, Russia*

ABSTRACT: An ultralight free scalar field with mass around $10^{-23} - 10^{-22}$ eV is a viable dark matter candidate, which can help to resolve some of the issues of the cold dark matter on sub-galactic scales. We consider the gravitational field of the galactic halo composed out of such dark matter. The scalar field has oscillating in time pressure, which induces oscillations of gravitational potential with amplitude of the order of 10^{-15} and frequency in the nanohertz range. This frequency is in the range of pulsar timing array observations. We estimate the magnitude of the pulse arrival time residuals induced by the oscillating gravitational potential. We find that for a range of dark matter masses, the scalar field dark matter signal is comparable to the stochastic gravitational wave signal and can be detected by the planned SKA pulsar timing array experiment.

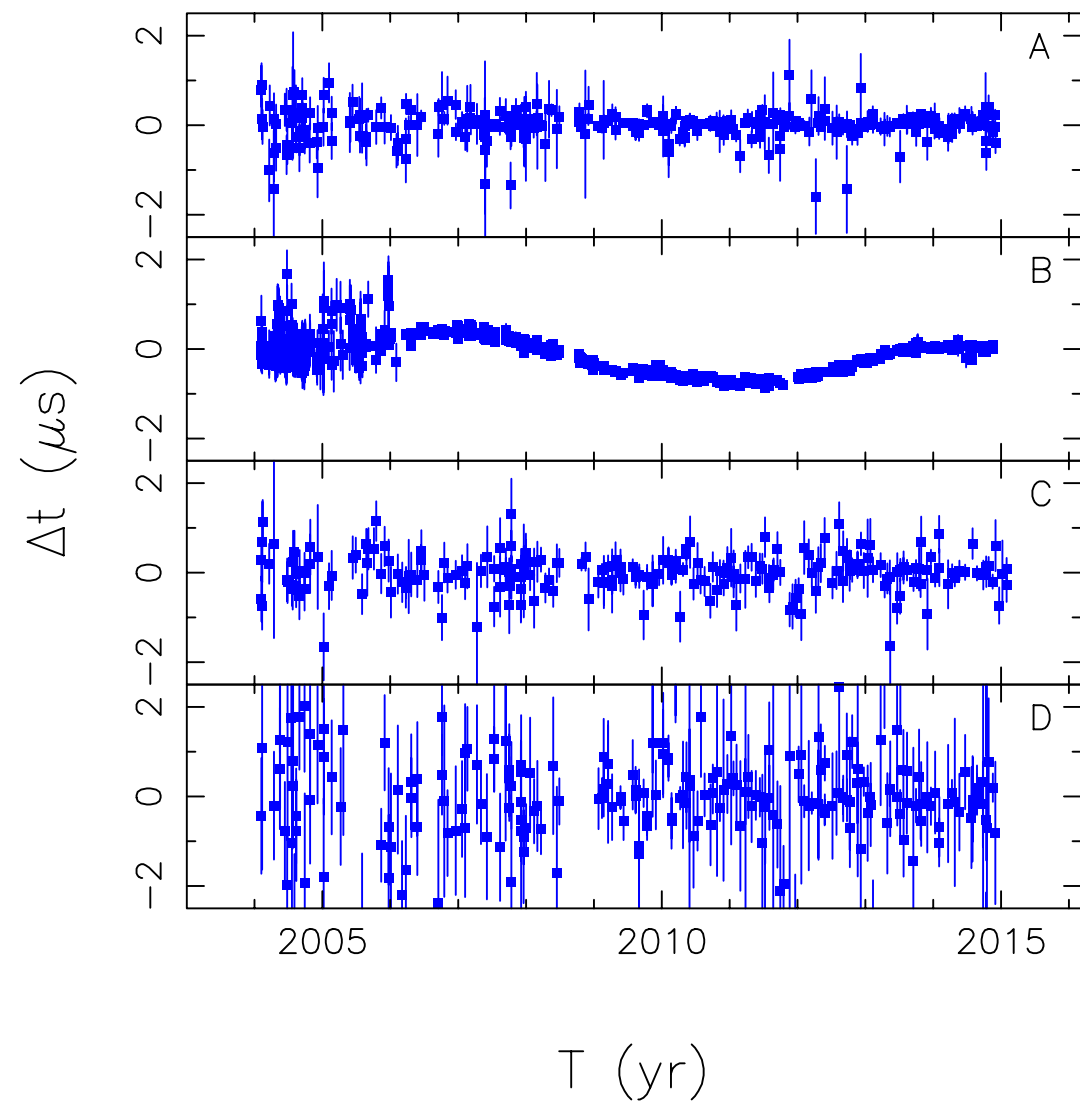
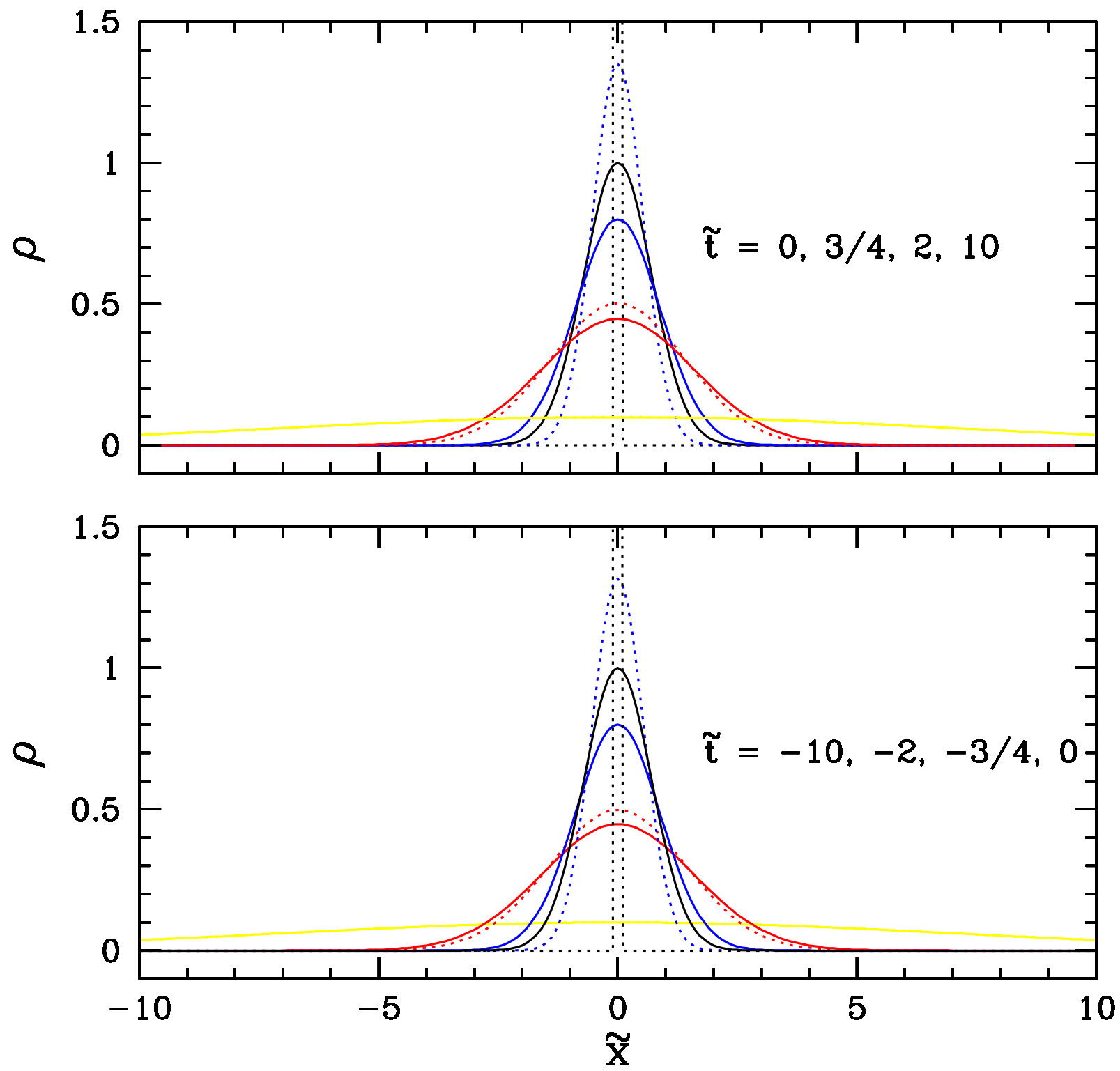


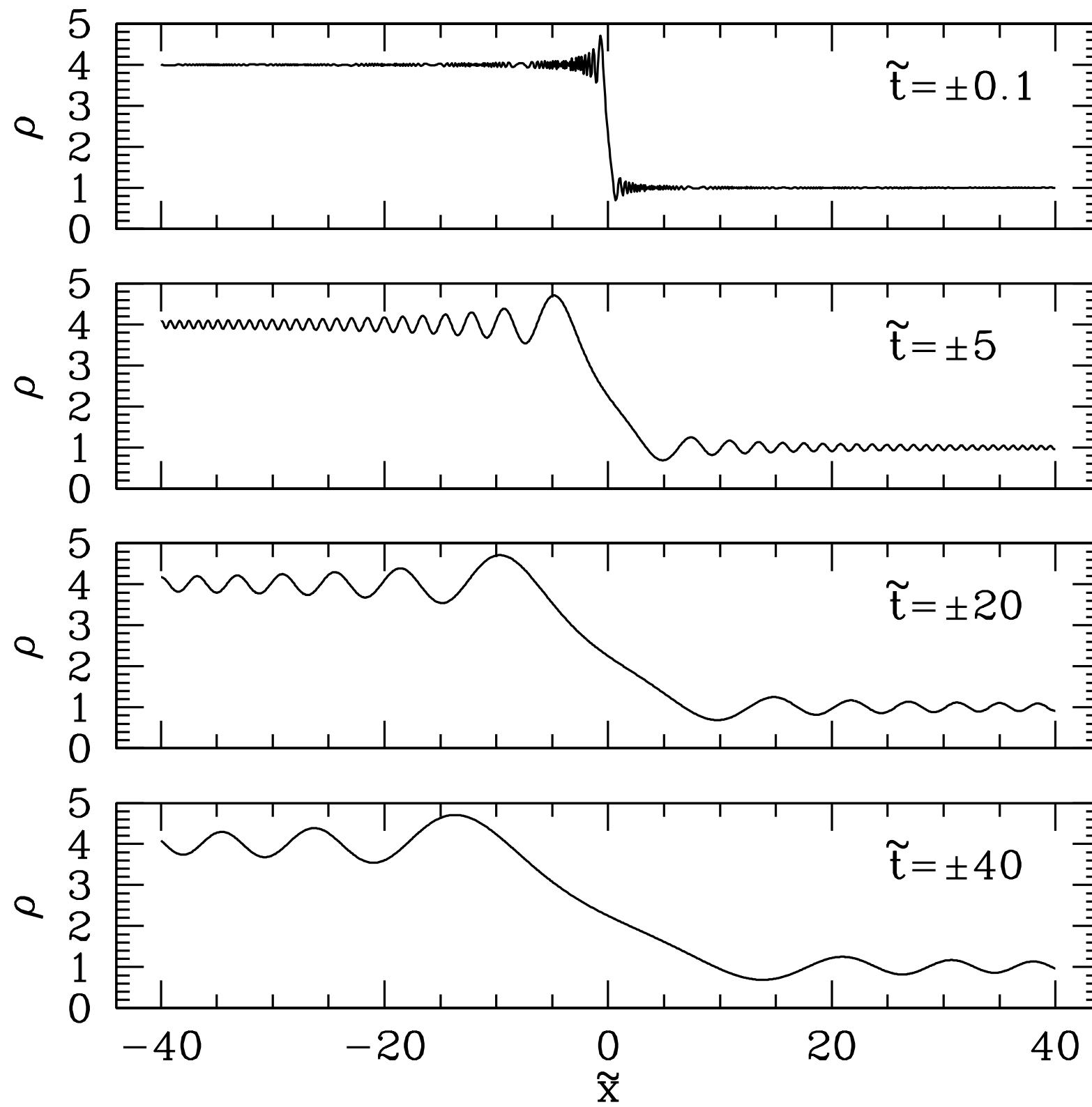
Fig. 1. Residual pulse times of arrival, Δt , for the four pulsars used in our analysis. These are PSR J1909-3744 (panel *A*), PSR J0437-4715 (panel *B*), PSR J1713+0747 (panel *C*), and PSR J1744-1134 (panel *D*).

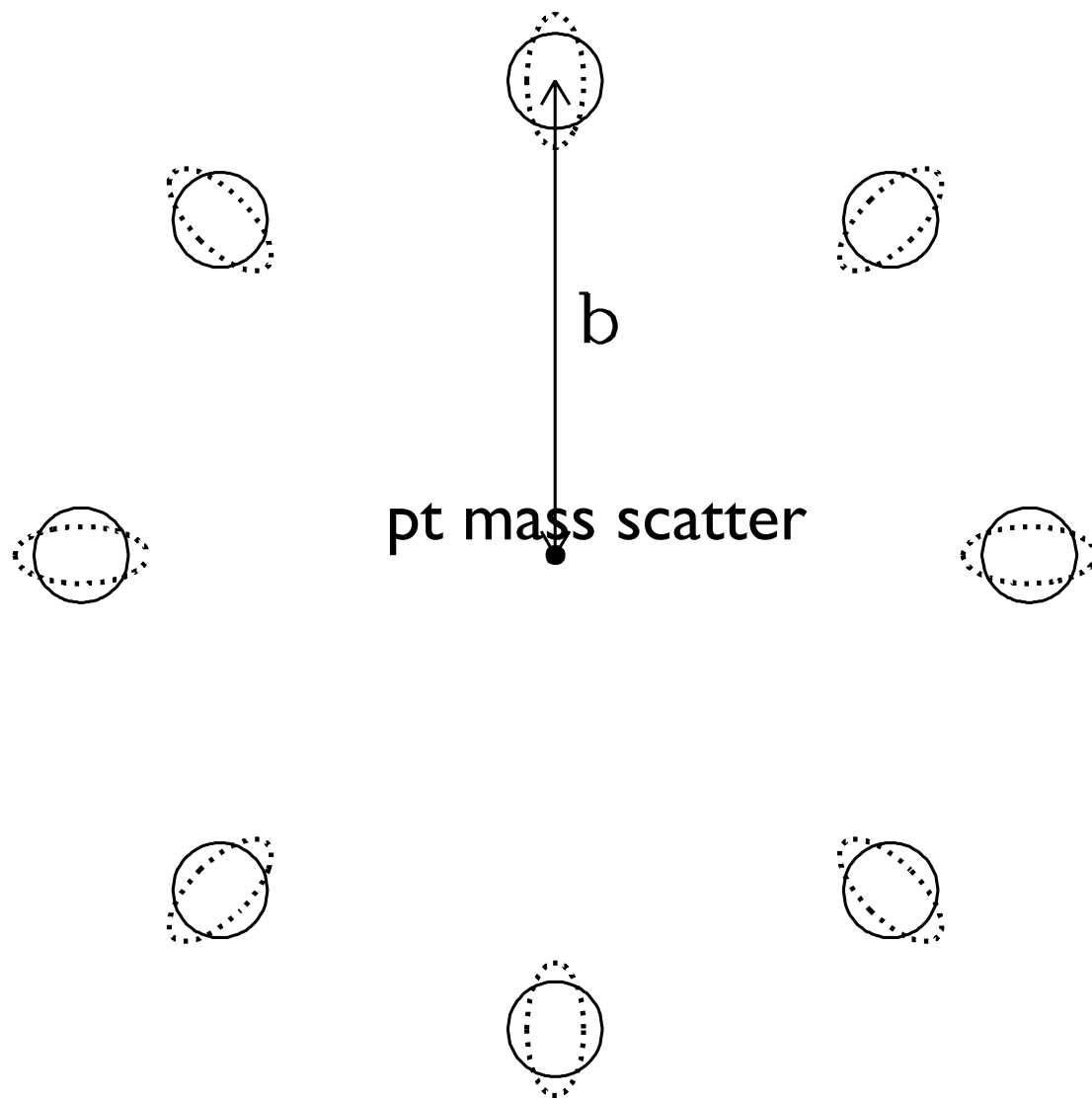
Shannon et al.

Possible diagnostics of FDM vs CDM:

- dynamical friction ✓
- evaporation of satellites by tunneling ✓
- interference ✓
- tidal streams & gravitational lensing ✓
- Lyman-alpha forest ✓
- direct detection
- detection by pulsar timing array ✓



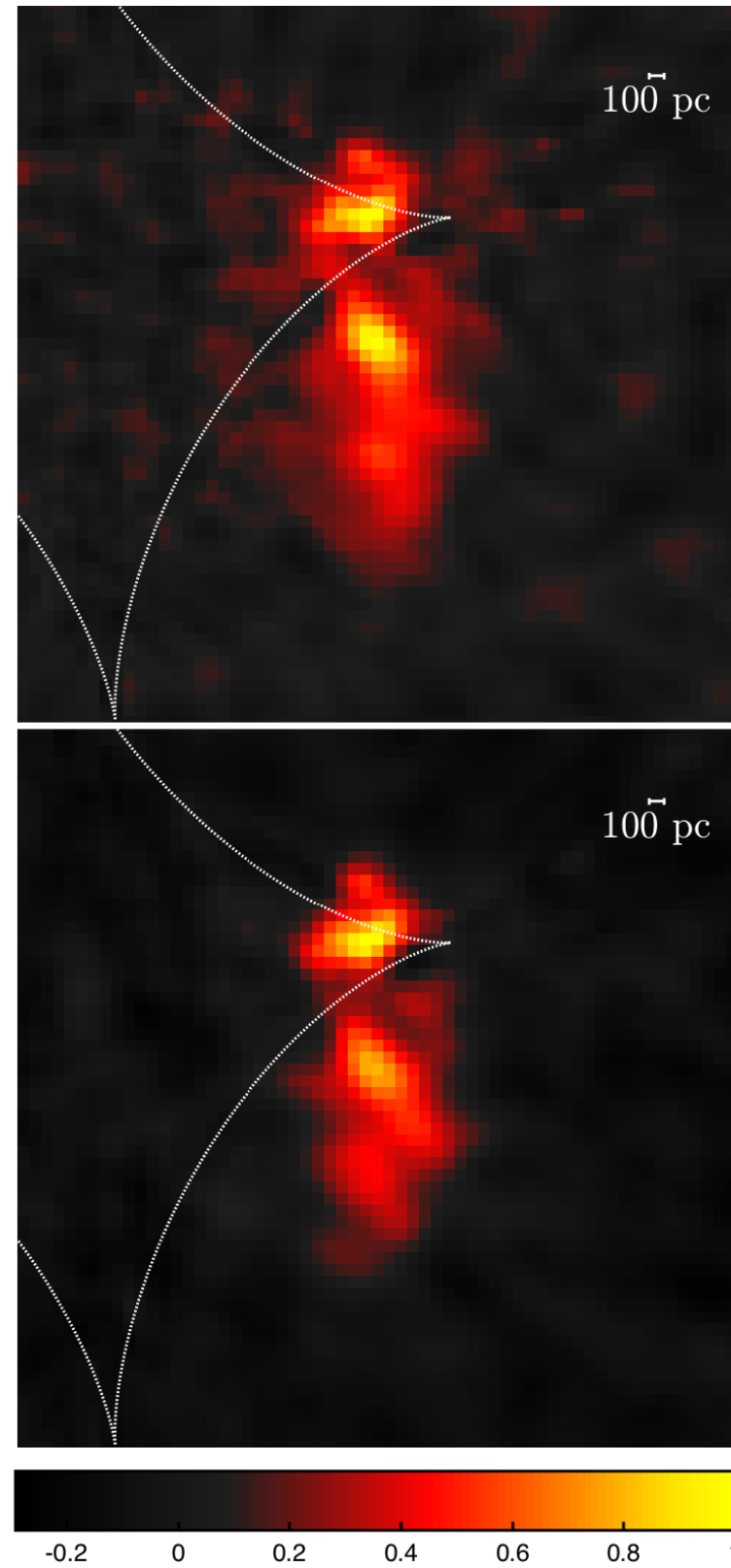




Average shear vanishes, but rms shear builds up in a random walk.

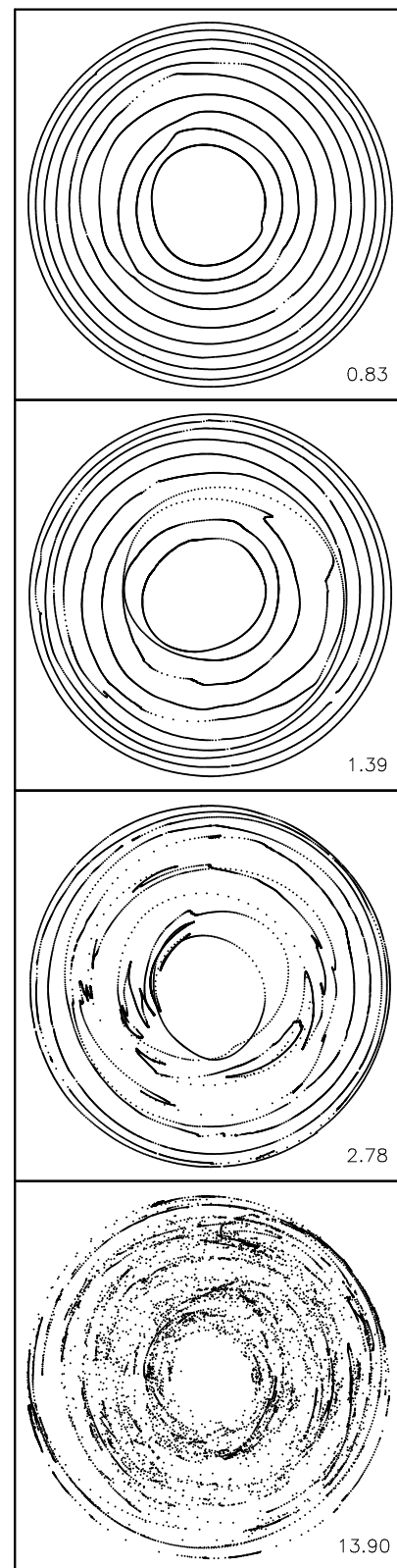
$$\text{rms shear of tidal stream} \sim N^{3/2} R^{-1} \int d^2 k_{\perp} P_{\delta}(k_{\perp})$$

where R = orbital radius, N = no. of orbits,
 P_{δ} = substructure power spectrum



Hezaveh, Dalal et al. ALMA

Figure 8. Reconstructed source continuum emission from Band 6 (top panel) and Band 7 (bottom panel) data on a 10 milli-arcsec pixel grid. The white dashed curve shows the tangential caustic predicted by our best-fit smooth model.



Carlberg 2009

FIG. 1.— Face on views of a time sequence within one simulation. A range of stream locations are sampled with ten rings with 1000 particles per ring. These idealized streams are initiated on purely circular orbits which would preserve their appearance in the absence of sub-halos. The time is shown in Gyr indicated in the lower right of each sub-panel. The plotted radii are the arctangent of the r_{max} scaled radii to allow a more uniform display. Note how a wave-like perturbation evolves into a z-fold which gradually leads to a scrambling of the ring.

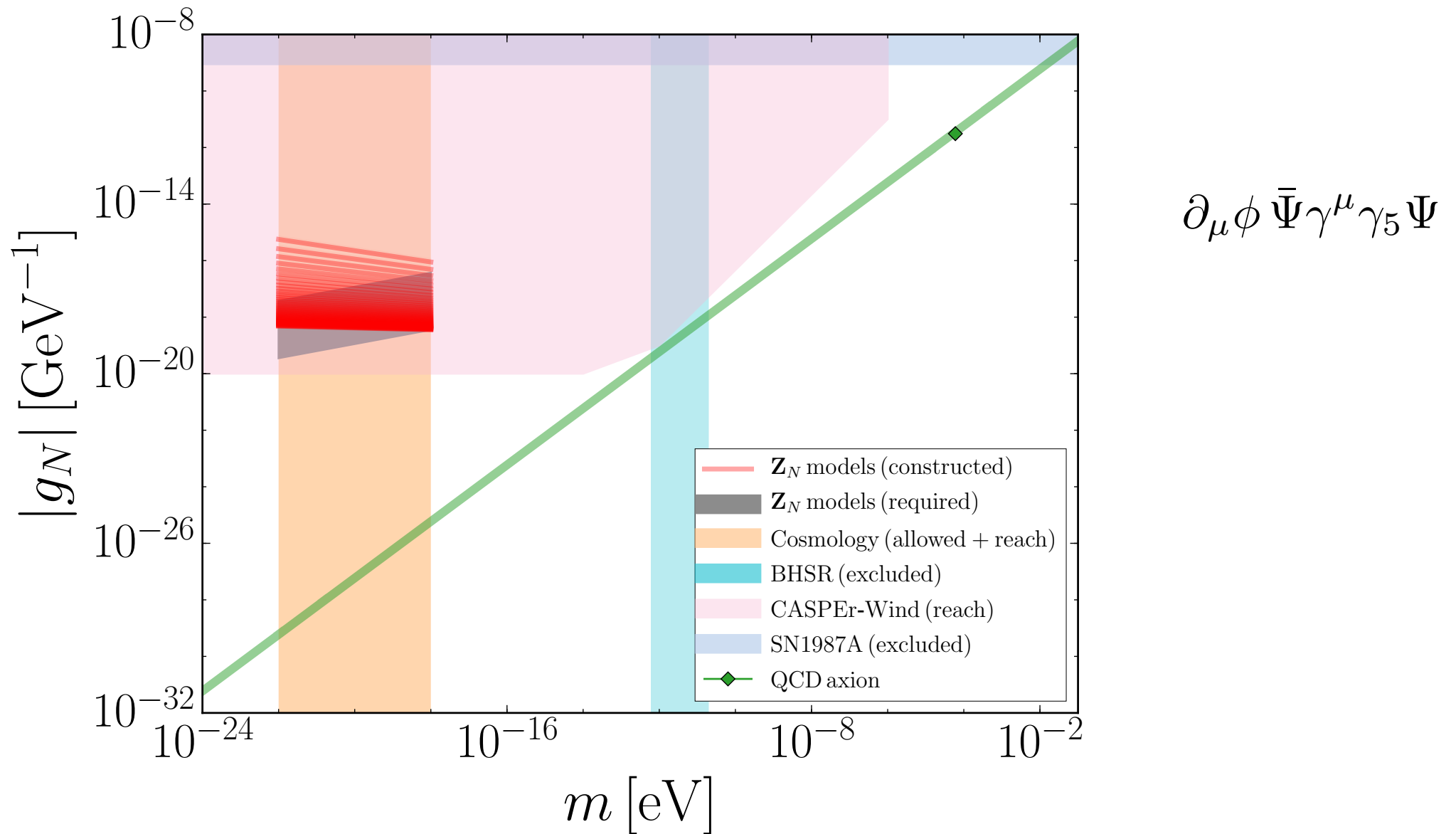
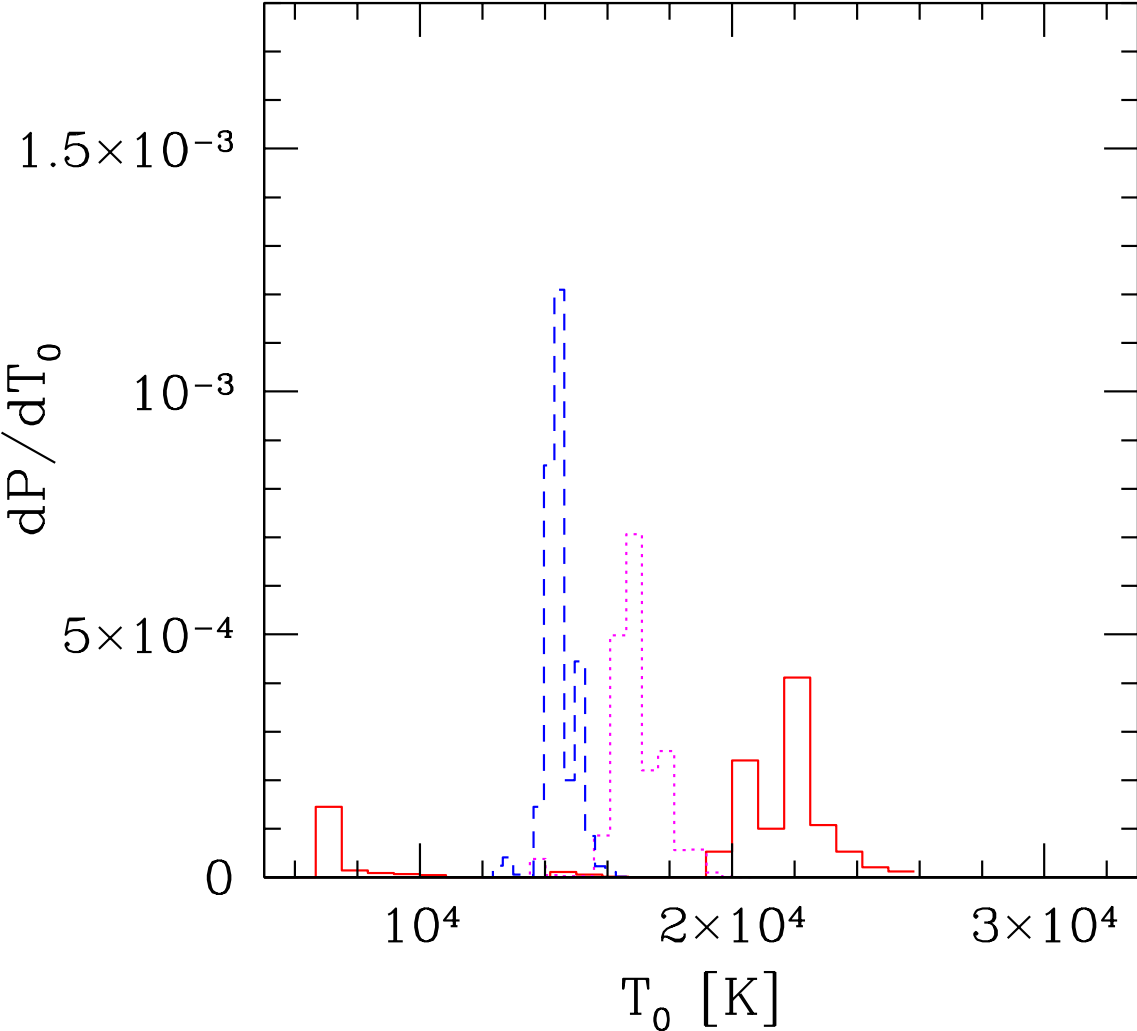


FIG. 3: Axion parameter space, (m, g_N) . The QCD axion paired with the ULA is shown for reference, along with the specific point $f_{\text{QCD}} = 10^{11}$ GeV, which is our reference value. BHSR excludes a range of masses at 2σ independent of DM abundance and coupling strength [76]. SN1987A excludes the shaded region with $g_N \gtrsim 8.2 \times 10^{-10}$, independent of DM abundance and axion mass [79]. The region both allowed and detectable using cosmology, and relevant to the small-scale crises of CDM is 10^{-22} eV $\lesssim m \lesssim 10^{-18}$ eV [24–26, 28–30]. We show the \mathbf{Z}_N models in this regime only, and also show the target region where f_{ULA} allows for the ULAs to be the dominant form of DM without fine tuning. The region accessible to direct detection using the spin precession technique of CASPER-Wind [34, 35] is also shown. The cosmologically relevant regime of the \mathbf{Z}_N models lies well within the projected sensitivity of CASPER-Wind, and is not excluded by any other probes.

Spread of temperature (at mean density) increases as $z \rightarrow$ reionization.



LH, Haiman